Electric dipole polarizability in ^{208}Pb: Insights from the droplet model

X. Roca-Maza,* M. Brenna, and G. Colò
Dipartimento di Fisica, Università degli Studi di Milano and INFN, Sezione di Milano, 20133 Milano, Italy

M. Centelles and X. Viñas
Departament d'Estructura i Constituents de la Matèria and Institut de Ciències del Cosmos (ICC), Facultat de Física, Universitat de Barcelona, Diagonal 645, 08028 Barcelona, Spain

B. K. Agrawal
Saha Institute of Nuclear Physics, Kolkata 700064, India

N. Paar and D. Vretenar
Physics Department, Faculty of Science, University of Zagreb, Zagreb, Croatia

J. Piekarewicz
Department of Physics, Florida State University, Tallahassee, Florida 32306, USA
(Received 17 July 2013; published 20 August 2013)

We study the electric dipole polarizability α_D in ^{208}Pb based on the predictions of a large and representative set of relativistic and nonrelativistic nuclear mean-field models. We adopt the droplet model as a guide to better understand the correlations between α_D and other isovector observables. Insights from the droplet model suggest that the product of α_D and the nuclear symmetry energy at saturation density J is much better correlated with the neutron skin thickness Δr_{np} of ^{208}Pb than the polarizability alone. Correlations of $\alpha_D J$ with Δr_{np} and with the symmetry energy slope parameter L suggest that $\alpha_D J$ is a strong isovector indicator. Hence, we explore the possibility of constraining the isovector sector of the nuclear energy density functional by comparing our theoretical predictions against measurements of both α_D and the parity-violating asymmetry in ^{208}Pb. We find that the recent experimental determination of α_D in ^{208}Pb in combination with the range for the symmetry energy at saturation density $J = [31 \pm (2)_{\rm est}]$ MeV suggests $\Delta r_{np}(^{208}\text{Pb}) = 0.165 \pm (0.009)_{\rm expt} \pm (0.013)_{\rm theor} \pm (0.021)_{\rm est}$ fm and $L = 43 \pm (6)_{\rm expt} \pm (8)_{\rm theor} \pm (12)_{\rm est}$ MeV.

DOI: 10.1103/PhysRevC.88.024316 PACS number(s): 24.30.Cz, 25.30.Bf, 21.60.Jz, 21.65.Ef

I. INTRODUCTION

Experimental and theoretical studies of isospin sensitive observables, such as the electric dipole polarizability, the neutron skin thickness, and the parity-violating asymmetry, are crucial for a better understanding of the isovector sector of the nucleon-nucleon effective interaction and for constraining present and future nuclear energy density functionals (EDFs) [1–3]. The isovector properties of the nuclear equation of state are governed by the nuclear symmetry energy. The symmetry energy $S(\rho)$ encodes the energy cost per nucleon in converting all the protons into neutrons in symmetric nuclear matter. Knowledge of the symmetry energy and of its density dependence is critical for understanding many properties of a variety of nuclear and astrophysical systems, such as the ground- and excited-state properties of nuclei [4], many aspects of heavy-ion collisions at different projectile-target asymmetries [5], and the structure, composition, and dynamics of neutron stars [6].

The electric dipole polarizability α_D in ^{208}Pb was recently measured at the Research Center for Nuclear Physics (RCNP) [1] via polarized proton inelastic scattering at forward angles. This experimental technique allows the extraction of the electric dipole response in ^{208}Pb over a wide energy range with high resolution [1]. By taking the average of all available data on the electric dipole polarizability in ^{208}Pb [7,8], a value of $\alpha_D = 20.1 \pm 0.6\,\text{fm}^3$ was reported [1]. This value, in combination with the covariance analysis performed for a given Skyrme functional [9], constrained the neutron skin thickness in ^{208}Pb to be $\Delta r_{np} = 0.156^{+0.025}_{-0.021}$ fm [1]. A subsequent systematic study based on a large class of EDFs was able to confirm the correlation between α_D and Δr_{np} [3]. This study extracted a neutron skin thickness $\Delta r_{np} = 0.168 \pm 0.022$ fm using the same experimental value of α_D.

The purpose of this paper is threefold. First, we resort to a macroscopic approach for describing the dipole polarizability, which enables one to qualitatively understand, in a simple and transparent way, the correlation between the electric dipole polarizability and the parameters that characterize the nuclear symmetry energy. Second, through a comprehensive ensemble of microscopic calculations performed with different types of EDFs [10–17] we provide a quantitative analysis which allows to define the regions where the experiment and the adopted microscopic approaches are compatible. Finally, the isospin properties of the considered EDFs are further investigated by the analysis of the dipole polarizability in combination with the parity-violating asymmetry measured in polarized elastic electron scattering.

*xavier.roca.maza@mi.infn.it

The paper is organized as follows. In Sec. II we introduce the microscopic and macroscopic models used in this work. In particular, we discuss some of the critical insights provided by the macroscopic droplet model. In the next section results are presented for the correlations between the electric dipole polarizability and both the neutron skin thickness and the parity-violating asymmetry. Finally, we offer our conclusions in Sec. IV.

II. THEORETICAL FRAMEWORK

In the present section we introduce the theoretical formalism that is used to compute the various observables studied in this work. In particular, we briefly review the mean-field plus random phase approximation (RPA) techniques used to compute the distribution of isovector dipole strength. Moreover, we make connection to the macroscopic droplet model (DM) and discuss the critical insights that emerge from such a simplified, yet powerful, description.

A. Microscopic models

For the theoretical calculations presented in this work we use a set of nonrelativistic and relativistic self-consistent mean-field models to predict ground-state properties of finite nuclei at either the Hartree-Fock or Hartree levels, respectively. These mean-field models have been accurately calibrated to fit a certain set of ground-state data, such as binding energies and charge radii of selected nuclei (including ^{208}Pb) as well as to a few empirical properties of infinite nuclear matter at, or around, saturation density. To deal with dynamic properties of the system, such as the electric dipole polarizability, the models adopt the linearization of the time-dependent Hartree or Hartree-Fock equations in a fully self-consistent manner. That is, the residual interaction employed in the calculation of the linear response is consistent with the one used to generate the mean-field ground state. This technique is widely known as the random phase approximation [18]. From the RPA calculations we obtain the distribution of the electric dipole strength $R(\omega; E1)$ by considering the dipole operator

$$\mathcal{D} = \frac{Z}{A}\sum_{n=1}^{N} r_n Y_{1M}(\hat{r}_n) - \frac{N}{A}\sum_{p=1}^{Z} r_p Y_{1M}(\hat{r}_p), \tag{1}$$

where N, Z, and A are the neutron, proton, and mass numbers, respectively; $r_{n(p)}$ indicates the radial coordinate for neutrons (protons); and $Y_{1M}(\hat{r})$ is the corresponding spherical harmonic. Using this definition of the dipole operator allows one to eliminate any contamination of the physical response from the spurious state [18,19]. Further details about these RPA calculations may be found in Refs. [9,15,17,20] and references therein. Once the electric dipole strength $R(\omega; E1)$ is determined as a function of the excitation energy ω, the dipole polarizability α_D can be computed as

$$\alpha_D = \frac{8\pi e^2}{9}\int_0^\infty \omega^{-1} R(\omega; E1)\, d\omega = \frac{8\pi e^2}{9} m_{-1}(E1), \tag{2}$$

where $m_{-1}(E1)$ is the sum of the inverse energy weighted strength.

B. Macroscopic model

The RPA formalism described above suggests that the extraction of the inverse energy weighted sum rule requires the evaluation of the full distribution of dipole strength $R(\omega; E1)$. However, given that only the m_{-1} moment is required—as opposed to the full distribution of strength—a significantly more efficient computation of the dipole polarizability relies on the so-called dielectric theorem [21,22]. In this case, one solves the ground-state problem associated with the model Hamiltonian $\mathcal{H}$ under the constraint of a weak one-body term of the form $\lambda\mathcal{D}$, where $\mathcal{D}$ is the dipole operator. That is, one searches for the constrained wave function $|\lambda\rangle$ solution of $\mathcal{H}' = \mathcal{H} + \lambda\mathcal{D}$. The dielectric theorem establishes that the m_{-1} moment can be computed from the expectation value of the Hamiltonian in the constrained ground state as

$$m_{-1}(E1) = \frac{1}{2}\left.\frac{\partial^2\langle\lambda|\mathcal{H}|\lambda\rangle}{\partial\lambda^2}\right|_{\lambda=0}. \tag{3}$$

Note that this represents an enormous simplification, as the constrained energy may be obtained from a mean-field calculation, without recourse to the RPA.

Applying the same type of procedure but solving the constrained problem classically by using the DM approach of Myers and Swiatecki [23], one obtains the following result:

$$\alpha_D^{\rm DM} = \frac{\pi e^2}{54}\frac{A\langle r^2\rangle}{J}\left(1 + \frac{5}{3}\frac{9J}{4Q}A^{-1/3}\right), \tag{4}$$

which was first derived by Meyer, Quentin, and Jennings [24]. In this equation $\langle r^2\rangle$ is the mean-square radius of the nucleus, J is the nuclear symmetry energy at saturation density, and Q is the so-called surface stiffness coefficient, which measures the resistance of neutrons against being separated from protons [23].

It was shown in Ref. [25] using a large set of EDFs that the ratio J/Q appearing in Eq. (4) is linearly related to the slope of the symmetry energy at saturation density L. Moreover, the DM gives the symmetry energy coefficient $a_{\rm sym}(A)$ of a finite nucleus of mass number A as follows [23,26]:

$$a_{\rm sym}(A) = \frac{J}{1 + \frac{9J}{4Q}A^{-1/3}}. \tag{5}$$

Expanding Eq. (5) to first order in the "small" parameter $JA^{-1/3}/Q$ [as was done in deriving Eq. (4)], we can write Eq. (4) as

$$\alpha_D^{\rm DM} \approx \frac{\pi e^2}{54}\frac{A\langle r^2\rangle}{J}\left(1 + \frac{5}{3}\frac{J - a_{\rm sym}(A)}{J}\right). \tag{6}$$

Given that the difference between J and $a_{\rm sym}(A)$ is directly related to the surface symmetry energy, the above result reveals that the electric dipole polarizability is sensitive to the ratio of the surface and bulk nuclear symmetry energies [27].

The DM may also be used to provide an expression for the neutron skin thickness in terms of a few bulk nuclear

properties [25,26,28]. That is,

$$\Delta r_{np}^{\rm DM} = \sqrt{\frac{3}{5}}\left[\frac{3r_0}{2}\,\frac{\frac{J}{Q}(I-I_C)}{1+\frac{9J}{4Q}A^{-1/3}}\right] + \Delta r_{np}^{\rm Coul} + \Delta r_{np}^{\rm surf}, \quad (7)$$

where $I \equiv (N-Z)/A$ is the relative neutron excess, r_0 is related to the saturation density ρ_0 by $\rho_0 = 3/(4\pi r_0^3)$, $I_C = (e^2Z)/(20JR)$, $R \equiv r_0 A^{1/3}$, $\Delta r_{np}^{\rm Coul} = -\sqrt{3/5}(e^2Z)/(70J)$ is a correction caused by the electrostatic repulsion, and $\Delta r_{np}^{\rm surf} = \sqrt{3/5}[5(b_n^2 - b_p^2)/(2R)]$ is a correction caused by the difference between the surface widths b_n and b_p of the neutron and proton density profiles [25,28].

In this manner, one may use the DM to relate the dipole polarizability to the neutron skin thickness. For this purpose, one expands Eq. (7) to first order in $JA^{-1/3}/Q$ and finds after some algebra the following relation:

$$\alpha_D^{\rm DM} \approx \frac{\pi e^2}{54}\frac{A\langle r^2\rangle}{J}\left[1+\frac{5}{2}\frac{\Delta r_{np}^{\rm DM} - \Delta r_{np}^{\rm Coul} - \Delta r_{np}^{\rm surf}}{\langle r^2\rangle^{1/2}(I-I_C)}\right]. \quad (8)$$

Adopting a value of $J = 31 \pm 2$ MeV as a reasonable estimate compatible with recent compilations [4,29], one finds for ^{208}Pb that $I_C \approx 0.028 \pm 0.002$ and $\Delta r_{np}^{\rm Coul} \approx -0.042 \pm 0.003$ fm. Moreover, in Ref. [30] it was shown that $\Delta r_{np}^{\rm surf} \approx 0.09 \pm 0.01$ fm for ^{208}Pb according to the predictions of a large sample of EDFs. Consequently, as a first reasonable approximation, one can neglect the small variations of I_C, $\Delta r_{np}^{\rm Coul}$, and $\Delta r_{np}^{\rm surf}$ in Eq. (8) and explicitly show that for ^{208}Pb the product $\alpha_D^{\rm DM} J$ is linearly correlated with $\Delta r_{np}^{\rm DM}$—in agreement with Ref. [27].

Given the well-known correlation between the neutron skin thickness of a heavy nucleus and the slope of the symmetry energy at saturation density $L \equiv 3\rho_0(dS/d\rho)_{\rho=\rho_0}$ implied by a large set of EDFs [31,32], one can also anticipate the emergence of a linear correlation between $\alpha_D J$ and L. To do so we rely on the findings of Ref. [26] that suggest that the symmetry energy coefficient of a finite nucleus is very close to that of the infinite system at an appropriate subsaturation density ρ_A [i.e., $a_{\rm sym}(A) \approx S(\rho_A)$]. Note that the density ρ_A approximately obeys the following simple formula:

$$\rho_A = \frac{\rho_0}{1+cA^{-1/3}}, \quad (9)$$

where c can be chosen so that $\rho_{208} = 0.1$ fm^{-3}. Using these results in Eq. (6) after expanding $S(\rho_A)$ around saturation density, namely,

$$a_{\rm sym}(A) \approx S(\rho_A) = J - L\epsilon_A + \cdots, \quad (10)$$

one arrives at

$$\alpha_D^{\rm DM} \approx \frac{\pi e^2}{54}\frac{A\langle r^2\rangle}{J}\left[1+\frac{5}{3}\frac{L}{J}\epsilon_A\right]. \quad (11)$$

Note that we have defined $\epsilon_A = (\rho_0 - \rho_A)/3\rho_0$, which is approximately equal to $\epsilon_A = 1/8$ for $\rho_0 = 0.16$ fm^{-3} for the case of ^{208}Pb. This formula suggests how J and L can be related if the dipole polarizability is known.

III. RESULTS

In this section we study correlations between the electric dipole polarizability (mostly in the form of $\alpha_D J$) and both the neutron skin thickness and parity-violating asymmetry in ^{208}Pb. Our microscopic analysis involves a large and representative body of EDFs. We employ nonrelativistic Skyrme EDFs widely used in the literature (labeled as Skyrme in the figures [10]) and six different families of systematically varied interactions produced, respectively, by a variation of the parameters around an optimal value (without significantly compromising the quality of the merit function). Two of the families are based on nonrelativistic Skyrme EDFs (labeled in the figures as SAMi [11] and SV [12]), while three families are based on meson-exchange covariant EDFs (labeled as NL3/FSU [13–15], and TF [16]). The last family is based on a meson-exchange covariant EDF but assuming density-dependent coupling constants (labeled as DD-ME [17]).

A. The dipole polarizability and the neutron skin thickness in ^{208}Pb

We start by displaying in Fig. 1(a) the dipole polarizability α_D as a function of the neutron skin thickness in ^{208}Pb as predicted by the large set of EDFs employed in this work. This figure is reminiscent of the corresponding Fig. 1 of Ref. [3] where a significant amount of scatter between the different calculations was observed, although a linear behavior was seen within each family of systematically varied interactions. These trends are confirmed in our figure that displays a correlation coefficient of only $r = 0.62$. Remarkably, the large spread in the model predictions is practically eliminated by scaling the dipole polarizability by J of the model. Indeed, the microscopic calculations shown in Fig. 1(b) support the correlation between $\alpha_D J$ and Δr_{np} as suggested by the DM approach, and clearly demonstrate—by comparing Figs. 1(a) and 1(b)—that $\alpha_D J$ is far better correlated to the neutron skin thickness of ^{208}Pb than the polarizability alone. Note that the correlation coefficient has increased all the way to $r = 0.97$.

The strength of the correlation shown in Fig. 1(b) allows one to reliably estimate, within the validity of our theoretical framework, the value of the neutron skin thickness of ^{208}Pb as a function of J—or vice versa—once the experimental value of $\alpha_D = 20.1 \pm 0.6$ fm^3 [1] is assumed:

$$\Delta r_{np} = -0.157 \pm (0.002)_{\rm theor} + [1.04 \pm (0.03)_{\rm expt} \pm (0.04)_{\rm theor}] \times 10^{-2} J, \quad (12)$$

where Δr_{np} is expressed in fm and J in MeV. The "expt" uncertainties refer to the propagation of the experimental uncertainty of α_D, whereas the "theor" uncertainties are associated with the confidence bands resulting from the linear fit shown in Fig. 1. The theoretical uncertainties are meant to indicate the region allowed by the employed EDFs. Moreover, adopting $J = [31 \pm (2)_{\rm est}]$ MeV as a realistic range of values for the symmetry energy [4,29] and combining this estimate with the measured value of the dipole polarizability [1], we extract from Fig. 1(b) the following constraint on the neutron

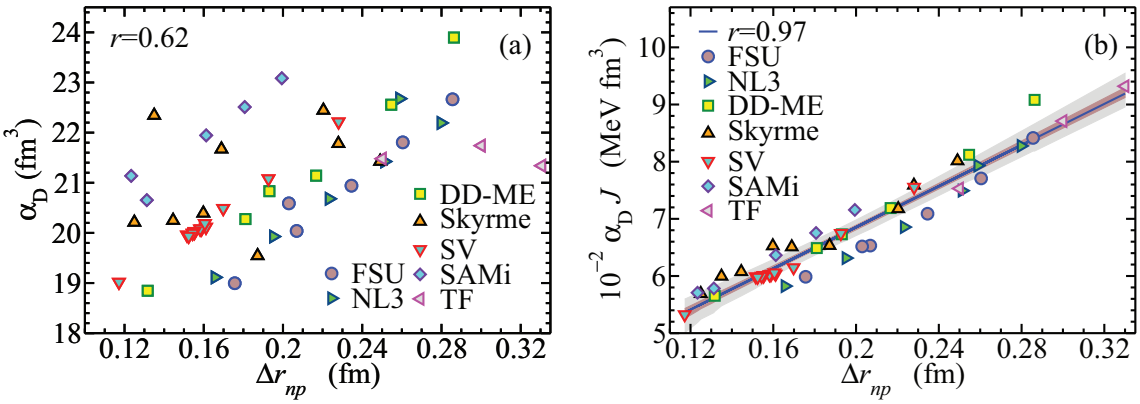

FIG. 1. (Color online) (a) Dipole polarizability against the neutron skin thickness in ^{208}Pb predicted by modern nuclear EDFs [10–17]. A correlation coefficient of $r = 0.62$ is found. (b) Dipole polarizability times the symmetry energy at saturation of each model against the neutron skin thickness in ^{208}Pb predicted by the same EDFs of panel (a). The linear fit gives $10^{-2}\alpha_D J = (3.01 \pm 0.32) + (19.22 \pm 0.73)\Delta r_{np}$ with a correlation coefficient $r = 0.97$, and the two shaded regions represent the 99.9% and 70% confidence bands.

skin thickness of ^{208}Pb:

$$\Delta r_{np} = 0.165 \pm (0.009)_{\rm expt} \pm (0.013)_{\rm theor} \pm (0.021)_{\rm est}\ {\rm fm}. \tag{13}$$

We labeled the uncertainty derived from the different estimates on J as "est" because it contains uncertainties coming from both experimental and theoretical analyses, which are often not easy to separate. In addition, we use a different label to keep track of the magnitude of the various uncertainties. Finally, we note that the above result for the neutron skin thickness of ^{208}Pb is in agreement with previous estimates [1–4,11,33].

Given the strong correlation between the neutron skin thickness of ^{208}Pb and the slope of the symmetry energy L, one expects that the strong correlation between $\alpha_D J$ and Δr_{np} will extend also to L. Moreover, based on the DM insights summarized in Eq. (11), we display in Fig. 2 the microscopic predictions for $\alpha_D J$ as a function of L for the same models depicted in Fig. 1. The correlation between $\alpha_D J$ and L is of particular interest since it provides a direct relation between J and L via the high-precision measurement of the electric dipole polarizability. Specifically, we obtain

$$L = -146 \pm (1)_{\rm theor} + [6.11 \pm (0.18)_{\rm expt} \pm (0.26)_{\rm theor}]J, \tag{14}$$

where both J and L are expressed in MeV. In particular, adopting as before a value of $J = [31 \pm (2)_{\rm est}]$ MeV, the above equation translates into the following constraint on L:

$$L = 43 \pm (6)_{\rm expt} \pm (8)_{\rm theor} \pm (12)_{\rm est}\ {\rm MeV}. \tag{15}$$

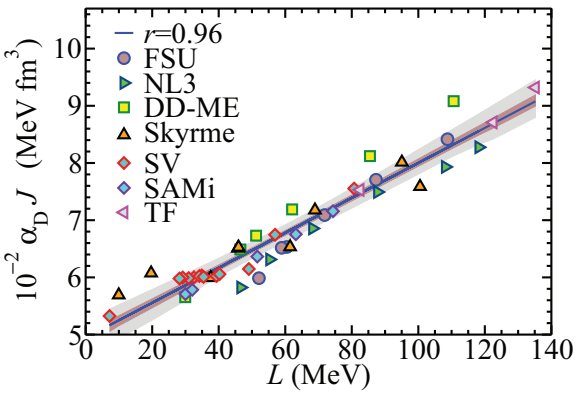

FIG. 2. (Color online) Dipole polarizability in ^{208}Pb times the symmetry energy at saturation as a function of the slope parameter L. The same EDFs [10–17] of Fig. 1 are used. The linear fit gives $10^{-2}\alpha_D J = (4.80 \pm 0.04) + (0.033 \pm 0.001)L$ with a correlation coefficient $r = 0.96$, and the two shaded regions represent the 99.9% and 70% confidence bands.

Our results show that the analytical formulas (8) and (11) reproduce the trends of the employed microscopic models. For completeness, we now evaluate the quantitative accuracy of these macroscopic formulas in reproducing the present self-consistent results. In doing so, we use the microscopic predictions for the different quantities appearing in the right-hand side of Eqs. (8) and (11) and calculate α_D by using the two macroscopic expressions. As a result, compared with the actual self-consistent values of α_D, we find that Eqs. (8) and (11) are accurate within 10% and 12% on average, respectively.

We conclude this section by noting that the analysis presented here may be systematically extended to other heavy nuclei if α_D is experimentally known. This could tighten the constraint between J and L.

B. The dipole polarizability and the parity-violating asymmetry in ^{208}Pb

The parity-violating asymmetry in the elastic scattering of high-energy polarized electrons from ^{208}Pb was recently measured at low momentum transfer at the Jefferson Laboratory by the Lead Radius Experiment (PREX) Collaboration [2]. The parity-violating asymmetry is defined as the relative difference between the differential cross sections of ultrarelativistic elastically scattered electrons with positive and negative

helicity [34]:

$$A_{\rm PV} = \left(\frac{d\sigma_+}{d\Omega} - \frac{d\sigma_-}{d\Omega}\right) \Big/ \left(\frac{d\sigma_+}{d\Omega} + \frac{d\sigma_-}{d\Omega}\right). \qquad (16)$$

This landmark experiment by the PREX Collaboration constitutes the first purely electroweak measurement of the neutron skin thickness of a heavy nucleus [2]. In a plane-wave Born approximation the parity-violating asymmetry is directly proportional to the weak-charge form factor of the nucleus—itself closely related to the neutron form factor. In exact calculations, where Coulomb distortions are taken into account, a highly linear relation has been found between $A_{\rm PV}$ and Δr_{np} in ^{208}Pb within the realm of nuclear EDFs (see Fig. 2 of Ref. [32]). The measured value of the parity-violating asymmetry at an average momentum transfer of $\langle Q^2 \rangle = 0.0088 \pm 0.0001$ GeV^2 reported by the PREX Collaboration is given by

$$A_{\rm PV} = 0.656 \pm (0.060)_{\rm stat} \pm (0.014)_{\rm syst} \text{ ppm}. \qquad (17)$$

The experimental uncertainty of 9% (dominated by the statistical error) is about three times as large as originally anticipated. By invoking some mild theoretical assumptions, the measurement of $A_{\rm PV}$ was used to extract the following value of the neutron skin thickness in ^{208}Pb [2,35]:

$$\Delta r_{np} = 0.302 \pm (0.175)_{\rm expt} \pm (0.026)_{\rm theor} \pm (0.005)_{\rm strange} \text{ fm}. \qquad (18)$$

The last contribution to the uncertainty is associated with the experimental uncertainty in the determination of the electric strange quark form factor. The result is consistent with previous estimates, although the central value is larger than the one extracted from the predictions of a large set of EDFs as well as from previous measurements of Δr_{np} in ^{208}Pb using hadronic probes [4]. We note, however, that one of the main virtues of an electroweak extraction of Δr_{np} is that it is free from most strong-interaction uncertainties. As mentioned, the main source of the experimental uncertainty in PREX arose from the limited statistics, and a new run PREX-II aiming at the original 3% accuracy in the determination of $A_{\rm PV}$ has been scheduled at the Jefferson Laboratory [36]. Moreover, parity-violating scattering experiments in ^{208}Pb with an even higher accuracy may be possible in the near future at the new MESA facility in Mainz [37].

Given the strong correlation displayed by both $\alpha_D J$ and $A_{\rm PV}$ with the neutron skin thickness of ^{208}Pb, it is natural to expect a close relation between $\alpha_D J$ and $A_{\rm PV}$. Note that the parity-violating asymmetry $A_{\rm PV}$ is the physical observable directly measured in the experiment. We display in Fig. 3 the predictions for $A_{\rm PV}$ at the PREX kinematics against $\alpha_D J$ for the same set of EDFs used in this work. Note that the nuclear physics input for $A_{\rm PV}$ involves both (point) neutron and proton densities—as opposed to only their respective rms radii—properly folded with the proton and neutron electromagnetic form factors. We underscore, however, that such densities are at the core of all nuclear density functionals, so the comparison against experiment may always be done directly in terms of $A_{\rm PV}$. Also shown in Fig. 3 are the regions allowed by the experimental data in the form of a horizontal band for PREX

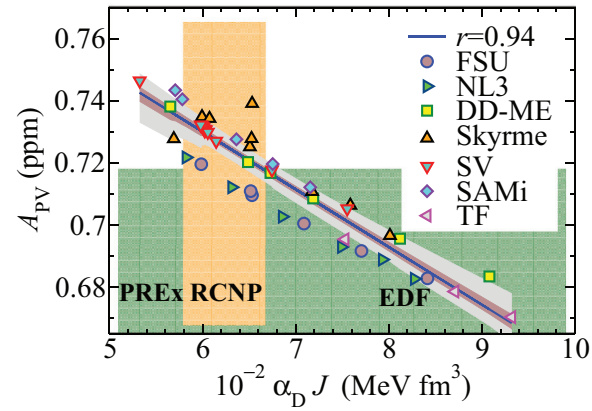

FIG. 3. (Color online) Parity-violating asymmetry in ^{208}Pb at the PREX kinematics as a function of dipole polarizability times the symmetry energy at saturation predicted by the same EDFs used in the previous figures [10–17]. The horizontal and vertical bands correspond to the region allowed by experimental data: $\alpha_D J = (6.23 \pm 0.44) \times 10^2$ MeV fm^3 and $A_{\rm PV} = 0.656 \pm (0.060)_{\rm stat} \pm (0.014)_{\rm syst}$ ppm. The linear fit gives $A_{\rm PV} = 0.842 \pm 0.001 - (186 \pm 10) \times 10^{-6} \alpha_D J$ with a correlation coefficient $r = 0.94$, and the two shaded oblique regions represent the 99.9% and 70% confidence bands.

[as given in Eq. (17)] and a vertical band for the RCNP measurement of α_D [$\alpha_D = 20.1 \pm 0.6$ fm^3], times an assumed value for the symmetry energy of $J = [31 \pm (2)_{\rm est}]$ MeV. That is,

$$\alpha_D J = [623 \pm (19)_{\rm expt} \pm (40)_{\rm est}] \text{ MeV fm}^3. \qquad (19)$$

Although there is some spread in the theoretical predictions, the large value of $r = 0.94$ suggests that the correlation between $\alpha_D J$ and $A_{\rm PV}$ remains strong. It is interesting to note that a more precise measurement of $A_{\rm PV}$ in ^{208}Pb with a central value lower than 0.7 ppm might rule out most (if not all!) of the state-of-the-art EDFs available in the literature. We stress that such a thought-provoking conclusion was reached by assuming a realistic range for the symmetry energy at saturation ($29 \leqslant J \leqslant 33$ MeV) compatible with different estimates [4,29]. Moreover, one may further constrain $A_{\rm PV}$ through its correlation with $\alpha_D J$. Indeed, invoking the experimental value for α_D with the alluded value for J leads to

$$A_{\rm PV} = 0.724 \pm (0.003)_{\rm expt} \pm (0.006)_{\rm theor} \pm (0.008)_{\rm est} \text{ ppm}. \qquad (20)$$

This would correspond to an accuracy of about 1.5%.

IV. CONCLUSIONS

In summary, we used insights from the droplet model to understand correlations between the electric dipole polarizability, the neutron skin thickness, and the properties of the symmetry energy around saturation density. The correlations suggested by the macroscopic droplet model were verified in a microscopic study using a comprehensive set of EDFs. In particular, we found that the product of the electric dipole polarizability α_D and the symmetry energy at saturation density J is a far better isovector indicator than α_D alone.

We showed that high-precision measurements of the dipole response of heavy nuclei (such as ^{208}Pb) can significantly improve our knowledge of the density dependence of the symmetry energy. Indeed, the strong correlation that we found between $\alpha_D J$ and the slope of the symmetry energy L was used to establish a tight relation between L and J [see Eq. (14)]. Moreover, by adopting the well-accepted range for the symmetry energy of $J = [31 \pm (2)_{\rm est}]$ MeV [4,29], the correlation between $\alpha_D J$ and the neutron skin thickness displayed in Fig. 1 suggests $\Delta r_{np} \approx 0.165$ fm for ^{208}Pb, with properly computed experimental, theoretical, and "estimated" uncertainties [see Eq. (13)]. Given the strong correlation between Δr_{np} and L, we were also able to constrain the slope of the symmetry energy at saturation density to $L \approx 43$ MeV. These values are consistent with the predictions for the neutron skin thickness in ^{208}Pb and L extracted from different experiments including heavy-ion collisions, giant resonances, antiprotonic atoms, hadronic probes, and spin polarized electron scattering (see Refs. [4,29] and references therein). They also agree nicely with the constraints on L and Δr_{np} of ^{208}Pb derived from recent astrophysical observations supplemented with microscopic calculations of neutron matter [38,39].

Furthermore, we found that the parity-violating asymmetry $A_{\rm PV}$ measured by the PREX Collaboration is strongly correlated not only with the neutron skin thickness but also with $\alpha_D J$. This has the advantage that theoretical calculations of $A_{\rm PV}$ may be directly compared against experiment—without the need to invoke (albeit mild) model-dependent assumptions. Ultimately, we have combined both observables ($A_{\rm PV}$ and α_D) to derive an experimentally allowed region for the theoretical models. The estimated uncertainties derived for L and Δr_{np} from the high-precision measurement of α_D are appreciably smaller than the ones expected from the 3% measurement of $A_{\rm PV}$ at PREX-II. Ideally, a 1% accuracy on $A_{\rm PV}$ may be required to improve the constraint already imposed from α_D [32]. However, we underscore that $A_{\rm PV}$ and α_D form a critical set of independent isovector indicators that could provide valuable insights into the nature of the nuclear density functional.

Finally, we highlighted the importance of performing high-precision measurements of α_D, and when possible $A_{\rm PV}$ [40], in other medium and heavy nuclei (e.g., ^{48}Ca, ^{120}Sn, and ^{208}Pb). We note that, whereas a large number of studies—including this one—suggest that the neutron skin thickness of ^{208}Pb is fairly thin, ruling out a thick neutron skin as suggested by the central value of the PREX experiment may be premature [16]. However, we are confident that systematic studies involving measurements of α_D and $A_{\rm PV}$ will help in constraining the density dependence of the symmetry energy. Thus, we encourage systematic studies of these observables as such a program will be of enormous value in constraining the isovector sector of the nuclear EDF.

ACKNOWLEDGMENTS

We are indebted to Professor W. Nazarewicz and Professor P.-G. Reinhard for valuable discussions. We also thank Professor P.-G. Reinhard for providing us with the results predicted by the SV family of interactions [12]. M.C. and X.V. thank Professor P. von Neumann-Cosel for useful correspondence. They acknowledge the support of the Consolider Ingenio 2010 Programme CPAN CSD2007-00042, Grant No. FIS2011-24154 from MICINN and FEDER, and Grant No. 2009SGR-1289 from Generalitat de Catalunya. Partial support from the U.S. Department of Energy under Contract No. DE-FG05-92ER40750 (J.P.) is greatly acknowledged.

[1] A. Tamii *et al.*, Phys. Rev. Lett. **107**, 062502 (2011).
[2] S. Abrahamyan *et al.* (PREX Collaboration), Phys. Rev. Lett. **108**, 112502 (2012).
[3] J. Piekarewicz *et al.*, Phys. Rev. C **85**, 041302 (2012).
[4] M. B. Tsang *et al.*, Phys. Rev. C **86**, 015803 (2012).
[5] B.-A. Li, L.-W. Chen, and C. M. Ko, Phys. Rep. **464**, 113 (2008).
[6] J. M. Lattimer and M. Prakash, Phys. Rep. **442**, 109 (2007).
[7] K. Schelhaas *et al.*, Nucl. Phys. A **489**, 189 (1988).
[8] A. Veyssiere, H. Beil, R. Bergere, P. Carlos, and A. Lepretre, Nucl. Phys. A **159**, 561 (1970).
[9] P.-G. Reinhard and W. Nazarewicz, Phys. Rev. C **81**, 051303 (2010).
[10] M. Bender, P.-H. Heenen, and P.-G. Reinhard, Rev. Mod. Phys. **75**, 121 (2003); P.-G. Reinhard, M. Bender, W. Nazarewicz, and T. Vertse, Phys. Rev. C **73**, 014309 (2006); L. G. Cao, U. Lombardo, C. W. Shen, and N. V. Giai, *ibid.* **73**, 014313 (2006); B. K. Agrawal, S. Shlomo, and V. Kim Au, *ibid.* **68**, 031304 (2003).
[11] X. Roca-Maza, G. Colò, and H. Sagawa, Phys. Rev. C **86**, 031306 (2012); X. Roca-Maza *et al.*, *ibid.* **87**, 034301 (2013).
[12] P. Klüpfel, P.-G. Reinhard, T. J. Bürvenich, and J. A. Maruhn, Phys. Rev. C **79**, 034310 (2009).
[13] G. A. Lalazissis, J. Konig, and P. Ring, Phys. Rev. C **55**, 540 (1997).
[14] B. K. Agrawal, Phys. Rev. C **81**, 034323 (2010).
[15] J. Piekarewicz, Phys. Rev. C **83**, 034319 (2011).
[16] F. Fattoyev and J. Piekarewicz, arXiv:1306.6034 [nucl-th].
[17] G. A. Lalazissis, T. Nikšić, D. Vretenar, and P. Ring, Phys. Rev. C **71**, 024312 (2005); D. Vretenar, T. Nikšić, and P. Ring, *ibid.* **68**, 024310 (2003).
[18] P. Ring and P. Schuck, *The Nuclear Many-Body Problem* (Springer, New York, 2004).
[19] K. Mizuyama and G. Colò, Phys. Rev. C **85**, 024307 (2012).
[20] G. Colò, L. Cao, N. V. Giai, and L. Capelli, Comput. Phys. Commun. **184**, 142 (2013).
[21] O. Bohigas, A. Lane, and J. Martorell, Phys. Rep. **51**, 267 (1979).
[22] L. Capelli, G. Colò, and J. Li, Phys. Rev. C **79**, 054329 (2009).
[23] W. D. Myers and W. J. Swiatecki, Ann. Phys. **84**, 186 (1974).
[24] J. Meyer, P. Quentin, and B. Jennings, Nucl. Phys. A **385**, 269 (1982).
[25] M. Warda, X. Viñas, X. Roca-Maza, and M. Centelles, Phys. Rev. C **80**, 024316 (2009).
[26] M. Centelles, X. Roca-Maza, X. Viñas, and M. Warda, Phys. Rev. Lett. **102**, 122502 (2009).
[27] W. Satuła, R. A. Wyss, and M. Rafalski, Phys. Rev. C **74**, 011301 (2006).
[28] W. D. Myers and W. J. Swiatecki, Nucl. Phys. A **336**, 267 (1980).

[29] J. M. Lattimer and Y. Lim, Astrophys. J. **771**, 51 (2013).
[30] M. Centelles, X. Roca-Maza, X. Viñas, and M. Warda, Phys. Rev. C **82**, 054314 (2010).
[31] B. A. Brown, Phys. Rev. Lett. **85**, 5296 (2000); R. Furnstahl, Nucl. Phys. A **706**, 85 (2002).
[32] X. Roca-Maza, M. Centelles, X. Viñas, and M. Warda, Phys. Rev. Lett. **106**, 252501 (2011).
[33] B. K. Agrawal, J. N. De, and S. K. Samaddar, Phys. Rev. Lett. **109**, 262501 (2012).
[34] C. J. Horowitz, Phys. Rev. C **57**, 3430 (1998); C. J. Horowitz, S. J. Pollock, P. A. Souder, and R. Michaels, *ibid.* **63**, 025501 (2001); D. Vretenar, P. Finelli, A. Ventura, G. A. Lalazissis, and P. Ring, *ibid.* **61**, 064307 (2000).
[35] C. J. Horowitz *et al.*, Phys. Rev. C **85**, 032501 (2012).
[36] PREX Collaboration, http://hallaweb.jlab.org/parity/prex/prexII.pdf
[37] C. Sfienti, talk given at the Workshop to Explore Physics Opportunities with Intense, Polarized Electron Beams up to 300 MeV and the Calcium Radius Experiment (CREX) Workshop at Jefferson Lab.
[38] A. W. Steiner, J. M. Lattimer, and E. F. Brown, Astrophys. J. **722**, 33 (2010).
[39] K. Hebeler, J. M. Lattimer, C. J. Pethick, and A. Schwenk, Phys. Rev. Lett. **105**, 161102 (2010); Astrophys. J. **773**, 11 (2013).
[40] S. Ban, C. J. Horowitz, and R. Michaels, J. Phys. G: Nucl. Part. Phys. **39**, 015104 (2012).